



Cite this: *Environ. Sci.: Atmos.*, 2024, **4**, 620

## Antimicrobial activity of safe concentrations of ozone, hydrogen peroxide, and triethylene glycol in air and surfaces

Joan Truyols-Vives, <sup>abc</sup> Salut Botella-Grau, <sup>d</sup> Josep Mercader-Barceló <sup>c</sup> and Herme G. Baldoví <sup>\*abc</sup>

Monitoring and control of indoor air hygiene has gained much interest since the COVID-19 pandemic because the airborne route is the main pathway for the spread of SARS-CoV-2 and other pathogens, making it necessary to develop strategies to mitigate airborne transmission of diseases. This work addresses indoor breathable air hygiene by proposing the *“in situ”* reduction of airborne microorganisms with the nebulization of low and safe concentrations of hydrogen peroxide ( $H_2O_2$ , 0.5 and 1 ppm), ozone ( $O_3$ , 0.06 and 0.2 ppm), triethylene glycol (TEG, 17.1, 52 and 171.2 ppm), and their combinations. The antimicrobial activity was evaluated in an office room by assessing the viability of commercial extremophile sporulated bacteria and naturally present bacteria and fungi in surfaces and air. All three chemicals individually dispersed reduced the viability of sporulated bacteria and naturally occurring microorganisms. Binary combinations were more effective than individual agents in the case of the  $H_2O_2$  and  $O_3$  mixture against sporulated bacteria, and the  $O_3$  and TEG mixture against airborne and surface bacteria. The ternary mixture was the most effective against commercial sporulated bacteria and airborne microorganisms. These results illustrate that the application of low and safe concentrations of antimicrobial compounds in indoor air could be an interesting strategy to reduce infection risk.

Received 31st October 2023  
 Accepted 9th April 2024

DOI: 10.1039/d3ea00156c  
[rsc.li/esatmospheres](http://rsc.li/esatmospheres)

### Environmental significance

Our work is a scientific answer to the question raised during the COVID-19 pandemic on how to treat indoor airborne droplets to stop disease transmission. To address this, we have studied the effectiveness of triethylene glycol (TEG) and breathable concentrations of  $O_3$  and  $H_2O_2$  against surface and airborne microorganisms (commercial spore strips and naturally occurring bacteria and fungi) in a real environment. The disinfection mechanism was investigated applying a novel method to identify the generated radical species in air. We found that TEG aerosols were especially effective over fungi. The dispersion of the ternary mixture significantly reduced the viability of airborne bacteria and fungi. This strategy might be useful to reduce infection risk through the airborne route in indoors.

## 1 Introduction

Indoor air is a natural reservoir of microorganisms that are present in small aqueous droplets suspended in air, termed bioaerosols.<sup>1</sup> Human activities such as talking, sneezing, and coughing generate bioaerosols.<sup>2,3</sup> In indoors, when agglomeration occurs, these actions increase microorganism populations. On average, a person breathes 14 m<sup>3</sup> of air per day,<sup>4,5</sup> this means that humans are daily exposed to many biological

pollutants. Some of the airborne microorganisms, including bacteria, fungi, viruses, and resistant vegetative sporulated forms, can be causative etiological agents of infectious diseases,<sup>4,6–8</sup> or even responsible for pandemic outbreaks such as the COVID-19.<sup>5,9–11</sup> Thus, respiratory infections represent a global health problem that causes thousands of deaths and the loss of millions of economic sources every year.<sup>12–14</sup> The identification and quantification of such agents is needed to assess the microbiological quality of indoor air and to estimate infection risk. In this context, fungi,<sup>15</sup> bacteria<sup>16</sup> and viruses, such as Influenza<sup>17</sup> and SARS-CoV-2 (ref. 18–20), have been detected in indoors. In addition to the development of technologies to monitor airborne microorganisms, it is also necessary to develop safe and effective strategies to reduce the viability of indoor microbiota in hot spots (*i.e.* overcrowded spaces with poor ventilation or healthcare centres),<sup>14,21</sup> thereby minimizing infection risk.

<sup>a</sup>Departamento de Química, Universitat Politècnica de València (UPV), 46022, Valencia, Spain. E-mail: [hergarba@cam.upv.es](mailto:hergarba@cam.upv.es)

<sup>b</sup>Instituto de Tecnología Química CSIC-UPV, Universitat Politècnica de València (UPV), 46022, Valencia, Spain

<sup>c</sup>Molecular Biology and One Health Research Group (MolONE), Universitat de les Illes Balears (UIB), 07122, Palma de Mallorca, Spain

<sup>d</sup>Departamento de Biotecnología, Centro Avanzado de Microbiología Aplicada (CAMA), Universitat Politècnica de València (UPV), 46022, Valencia, Spain



Several technologies are currently available for infection control in the food industry, wastewater treatment and surface cleaning,<sup>6,7,22,23</sup> while there is a lack of standardized protocols for disinfecting breathing air. Recently, researchers have focused on air treatment, by filtering or applying UV light, temperature, or others. In addition to them, the nebulization or dispersion of agents able to damage or destroy microorganisms in bioaerosols is a strategy with extensive possibilities. In this regard, there are several examples of chemical agents used to disinfect indoor environments. Some of the most used chemicals for this purpose are oxidant agents, such as HClO, O<sub>3</sub>, and H<sub>2</sub>O<sub>2</sub>, which are applied at high concentrations. For instance, concentrations higher than 200 ppm of O<sub>3</sub> are used to manufacture sterile products,<sup>24</sup> and H<sub>2</sub>O<sub>2</sub> concentrations ranging between 2 and 60 ppm are used to sterilize and disinfect medical equipment and facilities.<sup>25</sup> The antimicrobial efficacy of these compounds is due to their high oxidation capacity. As a drawback, exposure to high concentrations can cause strong irritability in the mucous membranes and lungs, limiting their application to non-occupied environments.<sup>24–26</sup> The antimicrobial potential of such agents has not been explored at lower concentrations on airborne microbiota and they might reduce the indoor microbial load. In agreement with this hypothesis, low O<sub>3</sub> concentrations (1.4 ppm) reduced the cell viability of pathogenic bacterial strains seeded on plates,<sup>27</sup> while exposure to 0.5% H<sub>2</sub>O<sub>2</sub> for a short period (5 minutes) was found to be virucidal and safe, since it was applied on persons without triggering acute inflammatory symptoms.<sup>28</sup> Against SARS-CoV-2, O<sub>3</sub> has been used to inactivate it in aerosols and fomites by using low concentrations, but above the limit of exposure.<sup>29</sup> Specially for SARS-CoV-2, oxidant agents are capable of destroying the proteins and lipids present in the envelope and the nucleic acids.<sup>30–32</sup>

Another family of chemicals with antimicrobial properties are biopolymers of glycol derivatives. Specifically, the antimicrobial potential of triethylene glycol (TEG) was demonstrated against Influenza virus strains at high concentrations.<sup>33</sup> The antimicrobial capacity of TEG could be due to its activity as a dehydrating agent.<sup>34,35</sup> TEG was found to be non-toxic even when the atmosphere is saturated with TEG,<sup>33,36</sup> and potential ecotoxicological effects are not reported.<sup>37</sup> Some authors have found that polyethylene glycol (PG), which is very similar to TEG from the chemistry standpoint, increases the fluidity of the viral membrane showing a broad effect on enveloped viruses such as SARS-CoV-2.<sup>38</sup> Moreover, as pure TEG is a dehydrating agent, it is reasonable to think that when TEG gets in contact with microorganism membranes, it will incorporate chemisorbed and physisorbed water molecules affecting arrangement of superficial proteins.

Furthermore, the combination of agents could increase the antimicrobial potential. In this regard, combinations of O<sub>3</sub> with H<sub>2</sub>O<sub>2</sub> have been tested,<sup>39</sup> but using concentrations that are above the exposure limits (Table 1), thereby impeding the application in occupied indoor spaces. Other mixtures such as fogging hypochlorous acid solution and hydrogen peroxide solution have been tested against SARS-CoV-2 and influenza A virus, being more efficient when they used together, and it was

found that SARS-CoV-2 was more resistant than Influenza A virus.<sup>40</sup> More recently, mixtures of peroxyacetic acid and hydrogen peroxide solutions have been investigated for airborne disinfection against SARS-CoV-2, with encouraging results.<sup>40</sup> The combination of antimicrobial agents with different mechanisms of action might allow a significant microbial reduction to be achieved without the need to raise the individual compound concentrations, thus allowing one to work even further away from the exposure limits of each compound. Although low concentrations of antimicrobial agents might be safe when applied separately, their behaviour must be analysed when applied in combination, including the formation of reactive oxygen species (ROS) by-products.

The antimicrobial activity of TEG, H<sub>2</sub>O<sub>2</sub> and O<sub>3</sub> has been evaluated mostly only under controlled conditions inside small and airtight chambers.<sup>27,39,47,48</sup> However, the results can differ when experiments are carried out in a real scenario. Thus, in the present work, we have analysed the chemical behaviour and the antimicrobial activity of the nebulization of low and safe concentrations of TEG, H<sub>2</sub>O<sub>2</sub> or O<sub>3</sub>, and their mixtures over commercial sporulated bacteria and naturally occurring bacteria and fungi in surfaces and in the air of a real scenario.

## 2 Materials & methods

### 2.1 Chemical compounds and equipment

The chemical compounds assayed were H<sub>2</sub>O<sub>2</sub> (30% w/w, Scharlau), TEG ReagentPlus® (99%, Sigma-Aldrich), and O<sub>3</sub> gas. The chemical reagents to measure TEG and H<sub>2</sub>O<sub>2</sub> in air were sulphuric acid (H<sub>2</sub>SO<sub>4</sub> 95–97%, J. T. Baker), potassium dichromate (K<sub>2</sub>Cr<sub>2</sub>O<sub>7</sub> 99%, Sigma-Aldrich), potassium titanium oxide oxalate dihydrate (C<sub>4</sub>H<sub>2</sub>K<sub>2</sub>O<sub>9</sub>Ti·2H<sub>2</sub>O, Sigma-Aldrich) and nitric acid (HNO<sub>3</sub> 68–70%, Scharlau). 5,5-Dimethyl-1-pyrroline N-oxide (DMPO, Sigma-Aldrich) and 2,2,6,6-tetramethylpiperidine (TEMP, Sigma-Aldrich) were used to determine radicals in air.

A GX500-EB ozone generator (ZonoSistem) and SM-41 ozone detector-controller (ZonoSistem) were employed to generate and measure O<sub>3</sub>, respectively. A Turbo-E 125 duct Fan (Blauberg Ventilatoren) was used to disperse the nebulized compounds through the room. A Microfogger 2-RC (Vosentech LLC) and LZ1500 Fog machine (LightSide) were used to nebulize TEG with the help of the turbo fan. A LKT170 Professional Nebulizer "NIXY Pro" (Moretti Spain) was employed to nebulize H<sub>2</sub>O<sub>2</sub>.

### 2.2 Chemical nebulization

Nebulization assays were performed in an office room as a model of a poorly ventilated indoor space. Dimensions of the room were 5.15 m × 3 m × 2.45 m with approximately 37.85 m<sup>3</sup>. The door and the window were closed while the assay was running. However, the room was not airtight as it was connected to the usual building ventilation system. Compounds were liberated at a height of 0.5 m from the ceiling, in a room corner and using a tube fan that recirculates the air. After reaching the desired airborne concentrations, compound concentrations were kept constant for 30 min.



Table 1 Exposure limits of chemicals used as references in this work

Chemical	Regulatory organism	<sup>e</sup> ppm	<sup>c,f</sup> mg m <sup>-3</sup>	Reference
Hydrogen peroxide (H <sub>2</sub> O <sub>2</sub> )	OSHA PEL <sup>a</sup>	1	1.4	41
	NIOSH REL <sup>b</sup>	1	1.4	42
	ACGIH TLV <sup>c</sup>	1	1.4	43
Ozone (O <sub>3</sub> )	OSHA 15 min exposure	0.3	0.6	44
	ACGIH EELV-DE <sup>d</sup>	0.2	0.4	45
	INSST EELV-DE <sup>d</sup>	0.2	0.4	46
Triethylene glycol (TEG)	OSHA PEL <sup>a</sup>	—	—	—
	NIOSH REL <sup>b</sup>	—	—	—
	ACGIH TLV <sup>c</sup>	—	—	—

<sup>a</sup> The PELs (Permissible Exposure Limits) are 8 hours TWA (time-weighted average concentration). <sup>b</sup> The RELs (Recommended Exposure Limits) are 10 hours TWA. <sup>c</sup> The TLVs (Threshold Limit Values) are 8 hours TWA. <sup>d</sup> The EELVs (Environmental Exposure Limit Values for Daily Exposure) are for heavy, moderate or light work for less than 2 hours. <sup>e</sup> Parts of vapor or gas per million parts of contaminated air by volume at 25 °C and 760 torr.

<sup>f</sup> Milligrams of substance per cubic meter of air. OSHA: Occupational Safety and Health Administration. NIOSH: National Institute for Occupational Safety & Health. ACGIH: American Conference of Governmental Industrial Hygienists. INSST: Instituto Nacional de Seguridad y Salud en el Trabajo.

### 2.2.1 One-compound nebulization

**2.2.1.1 TEG.** To study the antimicrobial activity of TEG, 0.8 mL or 2 mL of pure TEG liquid was nebulized with the Microfogger 2-RC at a flow rate of 0.24 g min<sup>-1</sup>. Larger quantities of TEG (6.5 mL) were nebulized with the LZ1500 Fog machine in 5 seconds. We observed that TEG aerosols were homogenized throughout the room after approximately 5 min. TEG concentration in the air was measured by passing 2 L of air through a gas trap charged with a TEG reactive solution, which was prepared with 0.068 M K<sub>2</sub>Cr<sub>2</sub>O<sub>7</sub> dissolved in 1 M H<sub>2</sub>SO<sub>4</sub>. TEG concentration was controlled by weighing the amount of TEG before and after nebulization to maintain a stable airborne concentration.

**2.2.1.2 O<sub>3</sub>.** Dosage of O<sub>3</sub> into the room was kept in the desired concentrations with continuous dosage using the SM-41 ozone detector-controller that measures and responds to real time O<sub>3</sub> concentration. The O<sub>3</sub> sensor was placed at 3.8 m distance from the O<sub>3</sub> generator, and at 1.6 m height. O<sub>3</sub> concentration was also measured with a personal gas detector WatchGas UNI O<sub>3</sub> (Casella) with a working range of 0 to 5 ppm, for double checking. O<sub>3</sub> was nebulized to achieve a concentration of 0.06 ppm and 0.2 ppm. The antimicrobial assay started when the O<sub>3</sub> levels were stabilized and then were kept stable for 30 min.

**2.2.1.3 H<sub>2</sub>O<sub>2</sub>.** The procedure to nebulize H<sub>2</sub>O<sub>2</sub> varied depending on the air concentration we wanted to reach. To reach 0.06 ppm, the H<sub>2</sub>O<sub>2</sub> nebulizer was charged with 5 mL of 10% (w/w) H<sub>2</sub>O<sub>2</sub> solution pH 5.4 until reaching 0.5 ppm. Then, it was turned off for ten minutes, switched on for ten minutes, and finally turned off for the last ten minutes of the assay. To reach 1 ppm, a 20% (w/w) H<sub>2</sub>O<sub>2</sub> pH 5.4 solution was charged and continuously nebulized for 30 min. H<sub>2</sub>O<sub>2</sub> concentration was measured with a colorimetric method by passing 28 L of air through a gas trap with a N86 LABOPORT Pump (KNF). The gas trap was filled with a 1 : 1 mixture of H<sub>2</sub>O<sub>2</sub> detection solution and deionized water. A 0.5 L stock H<sub>2</sub>O<sub>2</sub> detection solution was prepared by dissolving 200 mg (0.625 mmol) C<sub>4</sub>H<sub>2</sub>K<sub>2</sub>O<sub>9</sub>Ti·2H<sub>2</sub>O in a mixture of 14.5 mL of 95–97% H<sub>2</sub>SO<sub>4</sub>, 1 mL of 68–70%

HNO<sub>3</sub> and deionized water. The colorimetric method consisted of adding the “trapped liquid” in quartz cuvettes (Friedrich & Dimmock, Inc.) and measuring absorbance at 400 nm with a V-650 Spectrophotometer (Jasco).

**2.2.2 Two-compound nebulization.** The nebulisations of dual mixtures were performed for each case in the following order:

**2.2.2.1 O<sub>3</sub> + TEG.** First, 0.2 ppm O<sub>3</sub> was reached, and then 2 mL of TEG was evaporated.

**2.2.2.2 O<sub>3</sub> + H<sub>2</sub>O<sub>2</sub>.** After reaching 0.2 ppm O<sub>3</sub>, H<sub>2</sub>O<sub>2</sub> (20% w/w, pH = 5.4) solution was nebulized for 10 minutes until achieving 1 ppm concentration.

**2.2.2.3 3H<sub>2</sub>O<sub>2</sub> + TEG.** First, 1 ppm H<sub>2</sub>O<sub>2</sub> was reached, and then 2 mL of TEG was evaporated.

**2.2.3 Three-compound nebulization.** First, H<sub>2</sub>O<sub>2</sub> (20%, pH = 5.4) was nebulized for 10 minutes to reach 1 ppm concentration. Then, 0.2 ppm of O<sub>3</sub> and 2 mL of TEG were nebulized at the same time. Homogenic distribution of the TEG was determined visually and the concentration of O<sub>3</sub> was determined as explained before.

### 2.3 *In situ* antimicrobial assays

0.1 m<sup>3</sup> of air was sampled immediately before the nebulization of the compounds of interest and 30 min after reaching the desired concentrations. The antimicrobial assays were performed in May in the city of Valencia (Spain). Room temperature and humidity were monitored before and after each nebulization and were, on an average, 25 °C and 50 to 60% relative humidity. The culture of microorganisms was carried out following the national standard indications: UNE EN-ISO 4833-1:2013, UNE EN-ISO 4833-2:2013, UNE EN-ISO 7218:2008 and UNE EN-ISO 8199:2018.<sup>49–52</sup>

Air samples were collected with an Air Sampler SAS-Super100 (InstruLab S.C.) at a flow rate of 100 L min<sup>-1</sup>. The SAS sampler collects particles by impacting through a Petri dish containing Plate-Count (01-161-500, Scharlau) for bacteria, or Sabouraud (01-165-500, Scharlau) with Chloramphenicol Selective Supplement (06-118LY01, Scharlau) for fungi and yeast. Surface



samples were collected on a table at two points located at 2 and 4 m from the nebulizer. One rodac plate of Sabouraud and one rodac plate of plate-count were used to sample, respectively, fungi and bacteria by surface contact. These zones were cleaned and disinfected the night before each assay. Rodac plates and Petri dishes were incubated at  $30 \pm 1$  °C for 48–120 h  $\pm$  3 h. The colonies from air and surface samplings were counted manually with a colony counter. The results were given in percentage of reduction relative to the number of colonies arising from the samplings performed before the compound nebulization.

The assays with sporulated bacteria were performed using four spore strips containing a known quantity of *Geobacillus stearothermophilus* (Gke Steri-Record®). The strips were placed at a 1.7 m-height and at 3 m distance from the nebulization equipment. After the compound nebulization, the spore strips were introduced in tubes containing the spore culture media. The samples were mixed by vortexing for 5 minutes, sonicated for 10 minutes and, mixed for another 5 minutes to detach spores from the strips. The samples were incubated in a water bath at 85 °C for 1 minute. Under aseptic conditions, two dilutions were made from each tube. 100 mL of spore culture media dilutions were added to Petri dishes containing agar-dextrose-tryptone media (Difco) and spread with a Drigalsky handle to homogenize the bacteria through the Petri dishes. The dilutions were seeded in duplicate and incubated at 55 °C for 24–48 h. The colonies were counted manually with a colony counter and results were given in colony-forming unit per mL (CFU mL<sup>-1</sup>).

#### 2.4 Determination of radical species in air

The formation of airborne radicals was measured by nebulizing 0.2 ppm O<sub>3</sub>, 1 ppm H<sub>2</sub>O<sub>2</sub>, or the combination of both. Liquid-phase Electronic Paramagnetic Resonance (EPR) measurements were carried out using DMPO and TEMP as spin traps. Briefly, stock aqueous solutions of DMPO and TEMP (both at 1 mg mL<sup>-1</sup>) were prepared and, sequentially, 20 mL of each solution was introduced into the air trap. After 15 minutes of nebulization, we assumed that the airborne concentration of the chemical agents was stabilized, and then an air flow of 5.3 L min<sup>-1</sup> was induced with a N86 LABOPORT Pump for 5 min through the air trap charged with each solution. The samples were introduced into a vial where they were purged with argon for 5 minutes. A 5 mL aliquot was taken and measured on a Bruker EMS spectrometer (9.803 GHz, 3489.9 G scanning width, 40.95 ms time constant, 100 kHz modulation frequency, 1 G modulation width and 19.92 mW at 100 kHz microwave power).

#### 2.5 Statistical analysis

Graphical representations and statistical analyses were performed using GraphPad Prism 8. Data were represented as mean  $\pm$  standard error of the mean (SEM). Significant differences were determined by two-way ANOVA followed by the Bonferroni multiple comparison test and by Student's *t*-test. Differences were considered significant at  $P < 0.05$  (\*) and  $P < 0.005$  (\*\*).

## 3 Results and discussion

### 3.1 Environmental analysis of compound dosing

The compounds were nebulized and dispersed using a tube fan that projects an air stream parallel to the ceiling, and at the same time, induces recirculation of room air, helping to achieve a better homogenization of the chemicals. The chemicals were introduced in different ways: O<sub>3</sub> gas was generated "in situ", while pure TEG and H<sub>2</sub>O<sub>2</sub> were dispersed as aerosols.

Before proceeding with the antimicrobial experiments, the dispersion dynamics of the compounds were studied. For this purpose, the tube fan with the different dispensers was positioned in a corner of the office at different heights. The experiment was performed with all three chemicals but only the concentrations of H<sub>2</sub>O<sub>2</sub> and O<sub>3</sub> were easier to follow using the different sensors. When this experiment was performed with TEG, its distribution was assessed qualitatively by observing the light scattering produced by the TEG aerosols. Differences in the concentration of the chemicals were observed depending on the dosing height (Table 2). At 1.5 m height the air pressure pushed aerosols and gases downward, hampering the concentration homogenization (Fig. 1a). Even with TEG, gradients of light scattering were found to be denser at lower heights. In contrast, by projecting the aerosols at 2.5 m height, the chemicals were able to travel longer distances before landing on the walls, and a more homogenous dispersion was achieved for all chemicals (Fig. 1b). We attributed the better homogenization to the Coandă effect, in which fluids adhere to surfaces as they flow, in our case to the ceiling and walls. According to these results, the nebulization of the chemicals was set at a 2.5 m height for the antimicrobial assays.

Relative humidity is an environmental factor that influences microbial survival and proliferation. Therefore, we analysed the effect of compounds alone and combined at the concentrations selected to test the antimicrobial activities at relative humidity (Table 3).

The stability of the chemical concentrations in air was assessed 10 min after stopping the 30 min nebulisation (Table 3). We found out that TEG concentration loss was minimum. The case of O<sub>3</sub> was the opposite since the concentration rapidly dropped. This could be explained by its short lifetime of about few minutes in water<sup>57,58</sup> and hours in the gas phase.<sup>59,60</sup> As indicated by the high redox potential (Table 3), when O<sub>3</sub> meets any kind of surface or water aerosols, the gas rapidly reacts. O<sub>3</sub>

Table 2 Concentrations of O<sub>3</sub> gas and H<sub>2</sub>O<sub>2</sub> aerosols into the office room depending on the dosing height

Nebulization height (m)	Sampling height (m)	[O <sub>3</sub> ] ppm	[H <sub>2</sub> O <sub>2</sub> ] ppm
1.5	2.6	0.45	0.33
	1.6	0.2	1.6
	0.4	0.06	2.18
2.5	2.6	0.25	1.3
	1.6	0.2	1
	0.4	0.18	0.9



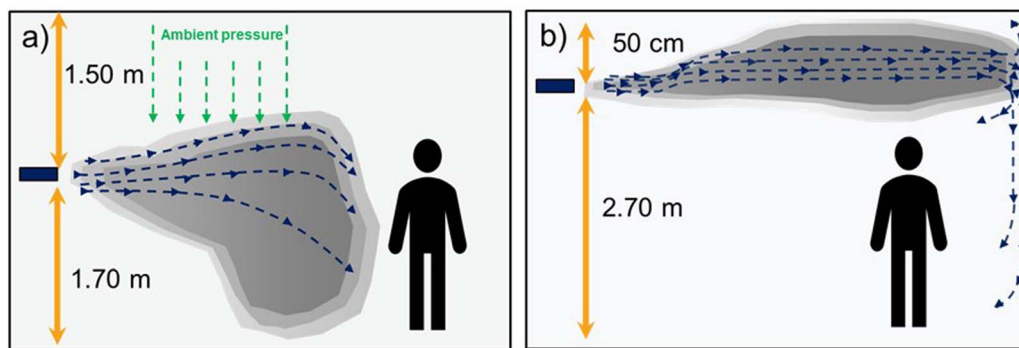


Fig. 1 Comparison of dosing  $O_3$  gas,  $H_2O_2$ , or TEG aerosols into the office room at (a) a medium height of about 1.5 m (without the Coanda effect), and (b) at 50 cm from the ceiling (at a height of 2.5 meters) with the Coanda effect.

is rapidly decomposed in water solution as the temperature, pH and stirring speed increase.<sup>53</sup> The decomposition rate of  $O_3$  in air is fast in indoor living areas because of the presence of objects and furniture that accelerate  $O_3$  decomposition.<sup>54</sup> On the other hand,  $H_2O_2$  aerosols showed an intermediate stability. The slightly acidic pH<sup>4,5</sup> of the solution we used could influence the stability of the molecule in air.<sup>56,61-64</sup> Thus, alkaline solutions promote decomposition of  $H_2O_2$  due to the increase of hydroxyl anions in solution, or even due to the deprotonation of  $H_2O_2$  itself. Another factor that it should be considered is high temperature, which could enhance  $H_2O_2$  degradation. However, as our working conditions are under 30 °C, herein the influence of this factor could be minor. In our case, the concentration drop could be mainly due to the impregnation into any type of surfaces, such as furniture, and the eventual fall of the heavier aerosols to the ground. Finally, a fact to be considered is the disappearance of 95% of TEG aerosols after 30 minutes when the three chemicals were dosed at the same time. This fact could be due to TEG degradation since it has been exposed to different reactive oxygen species (ROS) that eventually could completely degrade TEG to  $H_2O$  and  $CO_2$ .

### 3.2 Antimicrobial assays

The antimicrobial assays were conducted using commercial extremophile sporulated bacteria, and then with naturally

occurring indoor airborne and surface bacteria and fungi. The antimicrobial activities of the three chemical compounds and their mixtures were evaluated using concentrations that did not present adverse effects on human health upon long-time exposure. As the purpose of this work is to study the suitability of safe concentrations and eco-friendly chemicals to reduce natural bacteria and fungi populations in occupied spaces, the concentrations of  $H_2O_2$  and  $O_3$  were selected according to the guidelines of the INSST, NIOSH, ACGIH and OSHA, see Table 1. Following these criteria, we selected 0.2 ppm  $O_3$  and 1 ppm  $H_2O_2$ . International OSHA organism establishes a maximum safety exposure limit of 15 minutes at 0.3 ppm  $O_3$ ,<sup>44</sup> while INSST proposes a 0.2 ppm limit exposure for a time period of less than two hours.<sup>46</sup> Accordingly, we limited the  $O_3$  concentration to 0.2 ppm for 30 min. For  $H_2O_2$ , both organizations establish a limit of 1 ppm concentration<sup>54</sup> per hour, so we limited  $H_2O_2$  concentration to 1 ppm for 30 min. Moreover, lower concentrations of both chemicals were also tested to gain a better insight into their antimicrobial potential.

The selection of TEG concentration was not based on the guidelines since there is no defined airborne toxic concentration. However, we limited the TEG concentration to 171.2 ppm because higher quantities affect visibility.

**3.2.1 Reduction of sporulated bacteria.** The analysis of the antimicrobial potential of the candidate compounds under

Table 3 Summary of the chemical agent features nebulized alone and combined in an office room

Chemical	Redox potential <sup>a</sup>	Lifetime <sup>b</sup>	Concentration in the air <sup>c</sup>	Relative humidity change <sup>d</sup>	Concentration decrease <sup>e</sup>
TEG	—	Years	52 172	−6% −21%	<5%
$O_3$	2.07	From minutes in water <sup>f</sup> or to several minutes in air <sup>g</sup>	0.2	−10%	87%
$H_2O_2$	1.78	Months <sup>h</sup>	1	+ 5%	48%
$O_3 + TEG$	—	—	0.2 + 52	−17%	—
TEG + $H_2O_2$	—	—	52 + 1	−3%	—
$O_3 + H_2O_2$	—	—	0.2 + 1	−3%	—

<sup>a</sup> Volts at 25 °C in a vacuum. <sup>b</sup> Stability of pure TEG in the liquid phase,  $O_3$  in air and  $H_2O_2$  in 30% w/w aqueous solution. <sup>c</sup> Concentration in ppm.

<sup>d</sup> HR change measurement was done straightaway after stopping fogging. <sup>e</sup> Measured 10 minutes after stopping nebulization. <sup>f</sup> In water solution<sup>53</sup>

<sup>g</sup> In the gas phase.<sup>54</sup> <sup>h</sup> In aqueous solution.<sup>55,56</sup>



non-controlled conditions could produce inconclusive results because the daily environmental concentration of microorganisms is expected to vary from one day to another. Therefore, we first decided to use commercial spore strips loaded with a known amount of sporulated *G. stearothermophilus*.

The results in Fig. 2 show the viability reduction of *G. stearothermophilus* spores with different concentrations of the chemical compounds applied individually and combined. The nebulization of the lowest concentrations of the oxidant agents reduced the quantity of viable *G. stearothermophilus*, an effect that was dose-dependently enhanced. The most effective concentrations of oxidant agents were 0.2 ppm  $O_3$  and 1 ppm  $H_2O_2$ , achieving around 48% and 35% reduction, respectively ( $P = 0.025^*$  and  $P = 0.016^*$ , respectively). The increase of time exposure or concentration may result in a higher reduction, as was demonstrated by Andersen *et al.*, who completely eliminated the spore population contained in commercial strips located in rooms using up to 42 ppm of  $H_2O_2$  for longer periods than 30 min.<sup>25</sup> However, the use of such high doses precludes the presence of persons during nebulization.

The nebulization of TEG at 52 and 171.2 ppm led to a viability reduction of 68.1% and 56.7%, respectively, which were significantly higher compared to the 15.3% of reduction using 17.1 ppm ( $P = 0.001^{**}$  and  $P = 0.005^{**}$ , respectively). The nebulization of 52 ppm was the most effective TEG concentration and presented no significant differences compared to the highest concentration. Furthermore, 52 ppm TEG presented a higher viability reduction compared to 1 ppm  $H_2O_2$  or 0.2 ppm

of  $O_3$  ( $P = 0.008^{**}$  and  $P = 0.012^*$ , respectively). The efficacy of TEG aerosols to reduce *G. stearothermophilus* spore viability could be due to their dehydration capacity,<sup>34,35</sup> which somehow could inhibit the rehydration of the spores, showing an advantage compared to oxidant agents.

Afterwards, *G. stearothermophilus* spores were exposed to the combination of two and three compounds. Jeong *et al.* used a combination of  $H_2O_2$  and  $O_3$  at higher concentrations to obtain a complete disinfection in a chamber containing bacterial spore discs.<sup>36</sup> In our case, the combination of 0.2 ppm  $O_3$  and 1 ppm  $H_2O_2$  led to a 1.3- and 1.8-fold enhancement compared to the individual  $O_3$  and  $H_2O_2$  nebulisations, respectively. The viability reduction of the combination of 52 ppm TEG with 0.2 ppm  $O_3$  was not different (67.5%) from the reduction produced by TEG alone, while the combination of 52 ppm TEG with 1 ppm  $H_2O_2$  resulted in a lower reduction (44.7%) as compared to individual TEG. This result could be explained by the hydration of TEG aerosols by  $H_2O_2$  aqueous solution, and glycol-derived molecules act as stabilizers of  $H_2O_2$ , limiting its oxidation potential.<sup>65,66</sup> The most efficient combination in reducing *G. stearothermophilus* viability was the ternary mixture (69.5%), but this was not different from the binary TEG alone or in binary combination.

The fact that the viability reduction was not higher than 70% in any case may be, in part, related to how *G. stearothermophilus* spores are deposited in the strip. The spores are piled up on top of each other and this fact, together with the mild experimental conditions of atmospheric pressure and low concentrations of chemicals, makes it difficult to reach the spores deposited at the bottom of the dry drops. It should be pointed out that these commercial spores are prepared to guarantee disinfection efficacy in sterilization autoclaves where high pressures and temperatures are used.

Remarkably, the chemical compounds reduced a bacterial form of resistance even at low doses.<sup>67,68</sup> This result strongly suggests that low doses of the selected compounds could also eliminate significant quantities of vegetative cells and other less resistant microorganisms.

**3.2.2 Reduction of surface microorganisms.** The reduction levels of naturally occurring bacteria and fungi populations in indoors were measured by sampling horizontal surfaces before and after nebulizing the three compounds, alone and combined (Fig. 3). After the nebulisation of individual compounds, the viable bacterial population was reduced between 20 and 40% (Fig. 3a). In particular, the nebulisation of 0.2 ppm  $O_3$ , 1 ppm  $H_2O_2$  or 52 ppm TEG resulted in a reduction of bacterial population of about 26.8, 28.95 and 25%, respectively. The highest bacterial population reduction (57.1%) was obtained with the combination of 0.2 ppm  $O_3$  with 52 ppm TEG, thus indicating that their combination exerts an additive antibacterial effect. In contrast, the other two-compound combinations do not show any additive effect but, rather, the introduction of  $H_2O_2$  negatively affects the antibacterial effect of TEG. The three-compound nebulization exerted an antibacterial effect higher than the two  $H_2O_2$  binary combinations and the individual compounds.

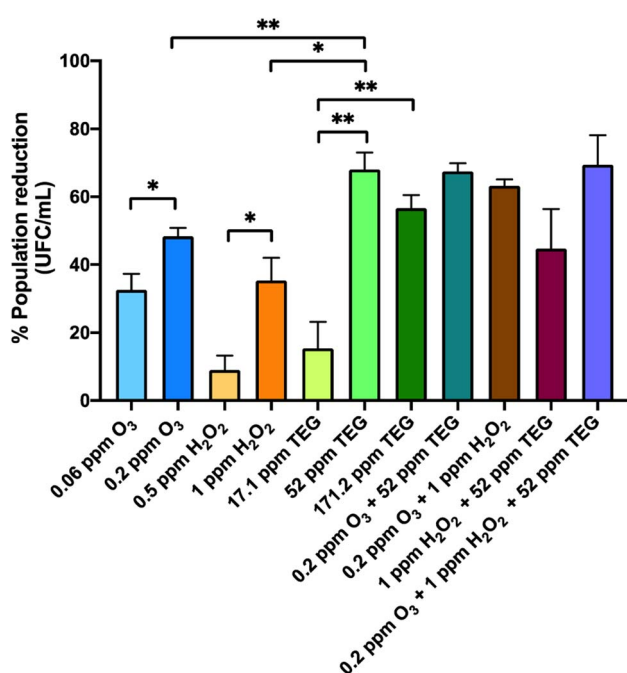


Fig. 2 Percentage of viability reduction of sporulated *G. stearothermophilus* after 30 minutes exposure to TEG,  $O_3$ ,  $H_2O_2$ , or their combinations. Plots represent percentage of reduction relative to the spore strips processed before the nebulization of any compound. Error bars indicate SEM.  $n = 3, 4$  or 8 per group. Significant differences were obtained by an unpaired two-tailed t-test  $*P < 0.05$ ,  $**P < 0.005$ .

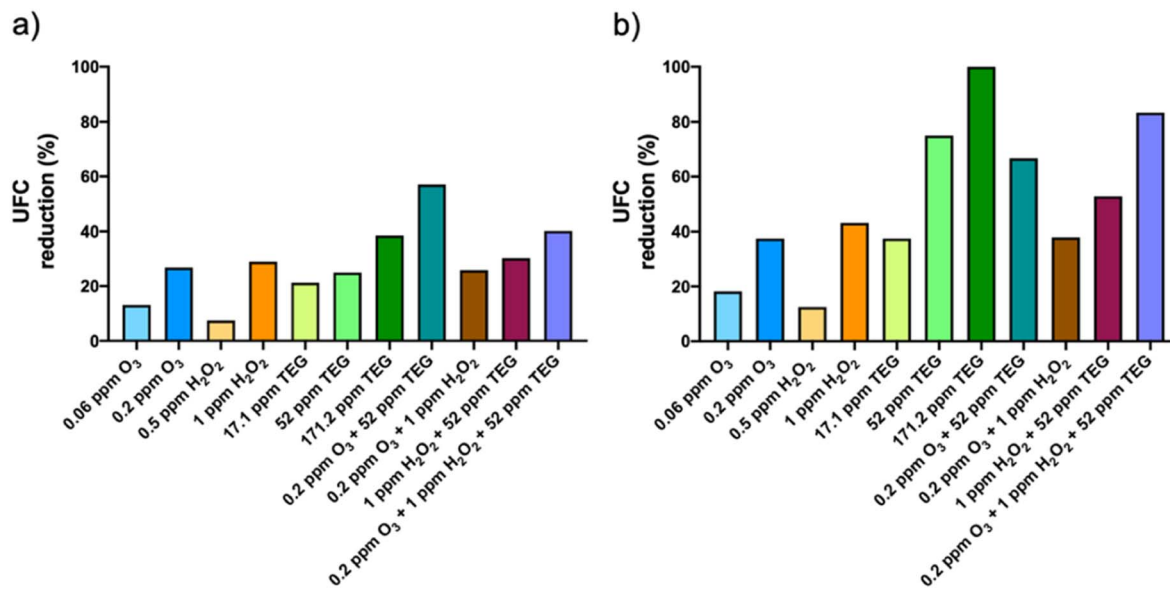


Fig. 3 Percentage of UFC reduction of (a) bacteria and (b) fungi over surfaces with triethylene glycol (TEG), ozone (O<sub>3</sub>) and hydrogen peroxide (H<sub>2</sub>O<sub>2</sub>) nebulized individually and combined. Plots represent percentage of reduction relative to the bacteria and fungi present before the nebulization of the compounds.

Surface fungi were found to be more sensitive to the selected chemicals than bacteria. As shown in Fig. 3b, the viability reduction produced by 0.2 ppm O<sub>3</sub> and 1 ppm H<sub>2</sub>O<sub>2</sub> was 37.5% and 43.1%, respectively. As in bacteria, TEG alone showed a higher antimicrobial activity than the oxidant agents, reaching 75% and 100% reduction with 52 ppm and 171.2 ppm TEG, respectively. The binary TEG combinations did not increase the antifungal effect of TEG dispersed alone. The combination of 0.2 ppm O<sub>3</sub> with 1 ppm H<sub>2</sub>O<sub>2</sub> did not increase the antifungal effects of the individual compounds either. The viability reduction of surface fungi was increased by combining O<sub>3</sub>, H<sub>2</sub>O<sub>2</sub> and TEG (83.4%) compared to all the binary mixtures, although such effect was lower than that produced by TEG alone.

The antimicrobial effects obtained by the oxidant agents are modest compared to those presented in other studies that were designed for disinfection purposes, in which higher concentrations or longer time exposures were used.<sup>24–26,29,47</sup> Despite that a complete viability reduction was not achieved in our study, a partial viability reduction of pathogenic microorganisms may entail a substantial reduction of infection risk. Moreover, the antimicrobial effects presented here could be further increased by extending the exposure time and/or combining with other antimicrobial agents as long as the experimental conditions are in agreement with the regulatory framework.

The differences in the antimicrobial activity between the binary TEG combinations could be explained in terms of solubility. While O<sub>3</sub> was dispersed pure in the gas phase, H<sub>2</sub>O<sub>2</sub> aerosols are made from a water solution. Since water has a higher solubility than O<sub>3</sub> in TEG aerosols, H<sub>2</sub>O<sub>2</sub> could react disintegrating them. In this way, O<sub>3</sub> and TEG will take longer to react compared to H<sub>2</sub>O<sub>2</sub> and TEG mixtures. In this sense, O<sub>3</sub> and TEG could work freely by promoting oxidation and dehydration

for longer periods of time. That could explain why TEG combined with O<sub>3</sub> has shown more optimal results.

**3.2.3 Reduction of airborne microorganisms.** The reduction of naturally occurring indoor airborne bacteria and fungi was assessed after nebulizing the compounds alone and combined. Results in Fig. 4a show that the individual nebulization of 0.2 ppm O<sub>3</sub>, 1 ppm H<sub>2</sub>O<sub>2</sub> and 52 ppm TEG resulted in 59.3%, 79.8% and 13% bacterial reduction, respectively. The reduction observed with H<sub>2</sub>O<sub>2</sub> is in accordance with the McCord *et al.* study, in which they used 1 ppm H<sub>2</sub>O<sub>2</sub> to reduce the transmission of *Clostridium difficile*.<sup>69</sup> The binary combination of 0.2 ppm O<sub>3</sub> with 52 ppm TEG reduced 82.1% of bacteria, showing an increasing efficacy compared to the individual compounds, as it occurred in commercial spores and surface bacteria. The combination of 0.2 ppm O<sub>3</sub> with 1 ppm H<sub>2</sub>O<sub>2</sub> reduced 79.6% of airborne bacteria, while the combination of 1 ppm H<sub>2</sub>O<sub>2</sub> with 52 ppm TEG presented a lower percentage of reduction compared to the other binary combinations, thus suggesting that TEG has been degraded by H<sub>2</sub>O<sub>2</sub> radicals.<sup>70</sup> When all three compounds were combined, the largest reduction (93.8%) of the airborne bacteria was produced, indicating that the ternary combination exerts an additive effect over airborne bacteria.

Airborne fungi were more sensitive to the tested chemicals than bacteria (Fig. 4b). In fact, the reduction of the fungal population was 100% with the highest O<sub>3</sub> and H<sub>2</sub>O<sub>2</sub> concentrations nebulized individually. 52 and 171.2 ppm TEG reduced the fungal population by 95% and 100%, respectively. The combinations of 52 ppm TEG with 0.2 ppm O<sub>3</sub> and 0.2 ppm O<sub>3</sub> with 1 ppm H<sub>2</sub>O<sub>2</sub> resulted in 88.9 and 100% reduction of the fungal population, respectively, while the 1 ppm H<sub>2</sub>O<sub>2</sub> with 52 ppm TEG was the binary combination that presented the



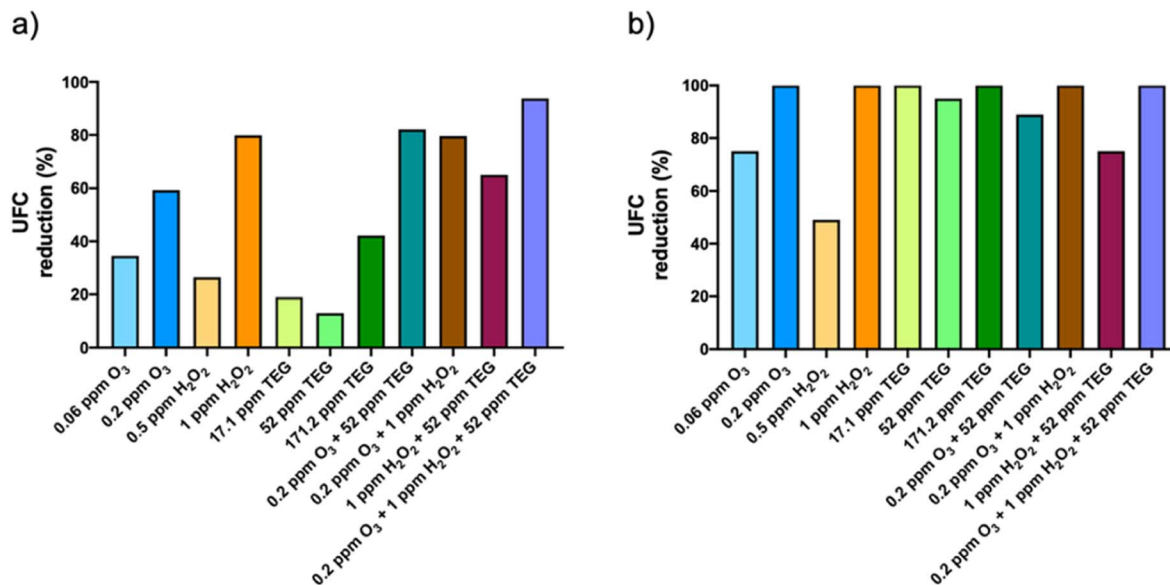


Fig. 4 Percentage of UFC reduction of airborne (a) bacteria and (b) fungi with triethylene glycol (TEG), ozone (O<sub>3</sub>) and hydrogen peroxide (H<sub>2</sub>O<sub>2</sub>) nebulized individually and combined. Plots represent percentage of reduction relative to the bacteria and fungi present before the nebulization of the compounds.

lowest antifungal activity (75%). Finally, the ternary combination resulted in a 100% reduction of the fungal population.

In summary, our work shows that the ternary mixture of O<sub>3</sub>, H<sub>2</sub>O<sub>2</sub> and TEG reduces the viability of more than 90% of the airborne microorganisms, an effect that was higher than that produced by the chemicals nebulized alone or in binary mixtures.

Our study presents several limitations. First, we mentioned that the assays were performed in a real scenario in which, however, some conditions were controlled, such as the lack of active ventilation. In real-life conditions, doors and windows are regularly opened and closed, and the air recirculation system and air conditioning units are working. In this case, the concentration of the nebulized chemical compounds will fluctuate and be diluted. Second, the concentrations of CO<sub>2</sub>, particulate matter, and volatile organic compounds, among other indicators of air ventilation were not measured. The collection of these data would have been useful in the context of this study. Finally, not all the bacteria and fungi species present in the room could be identified, whereas viruses were not analysed. The analysis on a broader range of microorganisms will provide a more complete picture of the antimicrobial potential of the candidate compounds. Future studies addressing the antimicrobial potential of safe concentrations of candidate compounds should consider these recommendations.

### 3.3 Chemical analysis of the nebulized compounds

**3.3.1 Detection of radical species with electron paramagnetic spectroscopy.** Next, we sought to identify the chemical-derived products formed after the nebulization of the investigated compounds, both alone and in combination, to help understand the underlying antimicrobial mechanisms and

assess the safety of nebulization. We employed electron paramagnetic resonance (EPR) spectroscopy to identify radical species in air samples by passing a certain volume of air into a gas trap that contains a molecular spin probe watery solution after nebulizing 1 ppm H<sub>2</sub>O<sub>2</sub>, 0.2 ppm O<sub>3</sub>, or their mixture.

The typical molecular spin probe used in chemistry to identify the presence of singlet oxygen species is TEMP, which reacts forming the TEMPO (2,2,6,6-tetramethylpiperidin-1-yl) oxyl adduct that can be identified by EPR spectroscopy.<sup>71,72</sup> Nebulization of H<sub>2</sub>O<sub>2</sub>, O<sub>3</sub> and H<sub>2</sub>O<sub>2</sub> + O<sub>3</sub>, showed the same EPR spectrum shape, containing three peaks at 3464, 3482 and 3497 G with intensity peak ratios of 1:1:1. In the literature, this characteristic TEMP signal is usually assigned to a TEMPO adduct that is formed when singlet oxygen is present in the sample.<sup>73,74</sup> In summary, these results indicate that the concentration of singlet oxygen increases, while H<sub>2</sub>O<sub>2</sub> and O<sub>3</sub> are decomposed. Since all samples were measured with the same experimental conditions, it is possible to estimate that O<sub>3</sub> nebulization generates twice the amount of singlet oxygen in comparison to H<sub>2</sub>O<sub>2</sub> nebulization. The nebulization of both oxidizing agents at the same time produces an increase in singlet oxygen concentration, however, its concentration is not significantly increased as it could be expected, meaning that the mixture of these compounds follows another chemical pathway.

Additionally, DMPO was utilized as a spin probe to determine other oxygen-derived radical species. In the case of O<sub>3</sub>, the EPR spectrum shows the appearance of 7 peaks that should correspond to the formation of more than one derived DMPO adduct (Fig. 5b). According to the literature, the 7 peaks could be grouped into two groups: the first one is formed by the 4 smaller peaks (3460, 3474, 3488 and 3503 G) with intensity ratios 1:2:2:1 corresponding to the presence of the 2,2-dimethyl-5-hydroxy-1-pyrrolidinyloxy (DMPO-OH) adduct, and



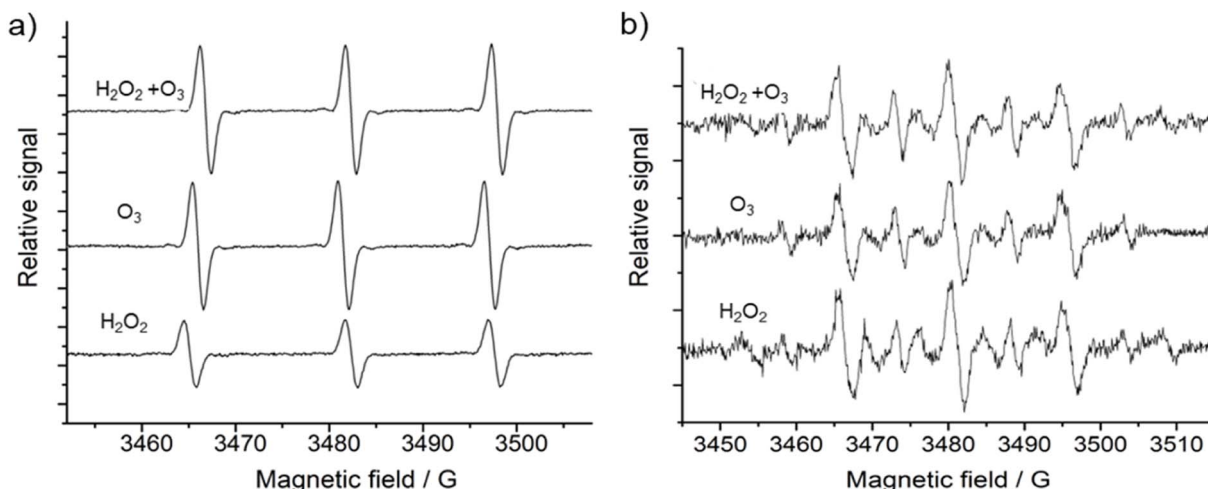


Fig. 5 EPR experimental spectra utilizing TEMP (a) or DMPO (b) as radical probes.

the second formed by the 3 bigger peaks (3465, 3480 and 3495 G) with ratios of 1 : 1 : 1 that corresponds to the overoxidized 5,5-dimethyl-2-oxo-pyrroline-1-oxyl (DMPOX).<sup>75</sup> The DMPO-OH adduct is produced when DMPO is exposed to hydroxyl radicals. This fact confirms that  $\text{O}_3$  also degrades to hydroxyl radicals probably by reacting with water molecules present in air. This interpretation agrees with the humidity reduction induced by  $\text{O}_3$  nebulization in Table 2. Accordingly, the exposure of DMPO solutions to a highly oxidative environment, for example the presence of  $\text{O}_3$  or singlet oxygen at the same time, over-oxidized them to DMPOX.<sup>75</sup>

However, when DMPO is exposed to  $\text{H}_2\text{O}_2$  aerosols, the EPR spectrum shows significant differences compared to the exposure to  $\text{O}_3$  (Fig. 5). Herein, the EPR spectrum of the  $\text{H}_2\text{O}_2$  sample shows 13 peaks instead of 7 found in the case of  $\text{O}_3$ . This new group of peaks means that an additional DMPO adduct has been produced. In this way, the 13 peaks have to be grouped into three different group peaks, corresponding to DMPO-OH and oxidized DMPOX, and the third group of peaks, with an intensity ratio of 1 : 1 : 1 : 1 : 1 : 1, is associated with the formation of the 2,2-dimethyl-5-hydroperoxy-1-pyrrolidinyl oxyl (DMPO-OOH) adduct.<sup>76</sup> With these data, we assume that nebulization of  $\text{H}_2\text{O}_2$  aqueous solutions produces  $\text{H}_2\text{O}_2$  aerosols that follow the common decomposition pathway through the formation of the hydroperoxyl radical, which rapidly forms hydroxyl radicals, and eventually will generate oxygen and water.

Finally, when  $\text{H}_2\text{O}_2$  aerosols and  $\text{O}_3$  gas were combined, EPR spectra of DMPO showed mainly the formation of DMPOX and DMPO-OH, but small traces of DMPO-OOH are detected. Importantly, the intensity of the peaks corresponding to the DMPO-OH adduct was higher than compared with individual nebulization of  $\text{H}_2\text{O}_2$ , meaning that the presence of the superoxide anion radical has been considerably reduced. Somehow,  $\text{O}_3$  is combined with  $\text{H}_2\text{O}_2$  and forces the decomposition of  $\text{H}_2\text{O}_2$  towards the hydroxyl radical.

**3.3.2 Discussion of the chemical decomposition mechanism of  $\text{H}_2\text{O}_2$ ,  $\text{O}_3$  and TEG in the air.** Inside the office  $\text{O}_3$ , the

concentration drops rapidly due to decomposition into several ROS molecules, following the fundamentals of stratospheric  $\text{O}_3$  reactions described by Chapman *et al.* producing molecular oxygen and atomic oxygen radicals,<sup>77</sup> see reaction (1). Usually, degradation of  $\text{O}_3$  takes place by photodissociation and thermal degradation<sup>77,78</sup> under the action of solar radiation inducing the formation of singlet oxygen that can be observed at any altitude near to ground level. In this way, it is reasonable to find that a certain percentage of the singlet oxygen detected by EPR in the office room comes from direct degradation of  $\text{O}_3$ , see reaction (2). Since tropospheric air composition is richer in water,<sup>79</sup> oxygen-derived radicals<sup>80</sup> coming from  $\text{O}_3$  self-degradation could react with water molecules, explaining the generation of hydroxyl radicals detected by EPR spectroscopy,<sup>79</sup> see reaction (3). In fact, the relative humidity registered in the model office room was always above 50%, favouring the reaction between water molecules and  $\text{O}_3$ .



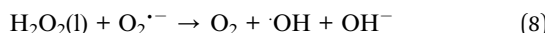
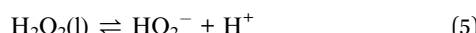
Either in water solution or the gas phase,  $\text{H}_2\text{O}_2$  seems to degrade to water and oxygen as shown in reaction (4),<sup>71,81,82</sup> but in the meantime it generates free radicals, many of them known as ROS. In water solutions,  $\text{H}_2\text{O}_2$  is considered as a weak acid, forming an acid-base equilibrium with the hydroperoxyl anion as shown in reaction (5), which will react with  $\text{H}_2\text{O}_2$  to form the hydroperoxyl radical (reaction (6)) that can establish an acid-base equilibrium forming the superoxide radical anion as proposed in reaction (7), which could react with  $\text{H}_2\text{O}_2$ , following the Haber-Weiss reaction,<sup>83</sup> see reaction (8). In our case, we nebulized a freshly prepared  $\text{H}_2\text{O}_2$  solution at pH 5.5, in which,  $\text{H}_2\text{O}_2$  should be relatively stable compared to more basic or acidic pHs.<sup>56</sup> However, once we generate the aerosols,  $\text{H}_2\text{O}_2$  molecules get in contact with high concentrations of  $\text{O}_2$



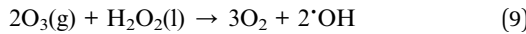
**Table 4** List of the redox potential of chemicals used and detected in the study

Product	Redox potential $E^\circ$ (V, 25 °C)
Hydroxyl radical ( $\cdot\text{OH}$ )	2.80 (ref. 87)
Ozone ( $\text{O}_3$ )	2.07 (ref. 88)
Hydrogen peroxide ( $\text{H}_2\text{O}_2$ )	1.78 (ref. 88)
Hydroperoxyl radical $\text{HO}_2^\cdot$	1.46 (ref. 87)
Oxygen singlet ( ${}^1\text{O}_2$ )	0.64 (ref. 87)

molecules, metal anion impurities,<sup>84</sup> airborne dust particles, bioaerosols or any solid surface<sup>85,86</sup> (e.g., furniture, wall paintings, room ceiling or ceramic floor) that will trigger  $\text{H}_2\text{O}_2$  degradation. Products of reactions (5) to (8) such as hydroperoxyl/superoxide radicals, hydroxyl radicals and singlet oxygen have been detected in EPR spectroscopy, demonstrating the self-decomposition of  $\text{H}_2\text{O}_2$  aerosols. The singlet oxygen molecule source could come from the oxygen molecules coming from  $\text{H}_2\text{O}_2$  degradation.

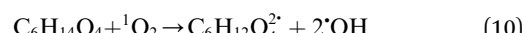


In the case of mixtures of  $\text{H}_2\text{O}_2$  and  $\text{O}_3$ , EPR spectroscopy experiments indicate the formation of hydroxyl and singlet oxygen species, indicating that the mixtures of  $\text{H}_2\text{O}_2$  aerosols and  $\text{O}_3$  gas promote the direct decomposition of  $\text{H}_2\text{O}_2$  molecules to hydroxyl radicals in air, see reaction (9). This fact agrees with Merényi *et al.* work that describes the perozone process, in which  $\text{H}_2\text{O}_2$  in water solution reacts with dissolved  $\text{O}_3$  gas, yielding hydroxy radicals and oxygen as main products.<sup>81</sup> Although little amounts of superoxide anion radicals are formed as an intermediate, they quickly react with  $\text{O}_3$  producing hydroxyl radicals. This will explain why in our case, the DMPO-OOH adduct signal is weakened when  $\text{O}_3$  and  $\text{H}_2\text{O}_2$  were mixed.<sup>81</sup> From the chemical standpoint, this fact can be explained since redox potentials of  $\text{O}_3$ ,  $\cdot\text{OH}$ , and  $\text{H}_2\text{O}_2$  are able to oxidate hydroperoxyl radicals to hydroxyl radicals, see potentials in Table 4. In this sense, the increment of  $\text{H}_2\text{O}_2$  decomposition rate due to the presence of strong oxidants, such as  $\text{O}_3$ , could explain the absence of increment in the antimicrobial activity of this binary mixture.



When TEG was fogged into the office room alone, or mixed with  $\text{H}_2\text{O}_2$  aerosols or  $\text{O}_3$ , it produced a light fog that was stable in air for a long period of time, but when equal concentrations of TEG were mixed with  $\text{H}_2\text{O}_2$  and  $\text{O}_3$  gas, 90% of initial TEG

was degraded. According to the literature,<sup>70,89</sup> when TEG molecules get contact with oxygen and hydroxyl radicals, it triggers TEG degradation, ending with the formation of  $\text{CO}_2$  and  $\text{H}_2\text{O}$ . In this specific case, the presence of singlet oxygen molecules triggers TEG degradation,<sup>90,91</sup> forming terminal hydroxyl functional groups and hydroxyl radicals, which react with this pre-oxidated TEG easily,<sup>37</sup> see reactions (10) and (11). Moreover, considering that TEG is a dehydrator agent, it is reasonable to think that in our case, TEG aerosols will incorporate ambient aqueous  $\text{H}_2\text{O}_2$  aerosols facilitating the degradation of TEG. This fact would explain why the ternary mixtures trigger the highest airborne antimicrobial activity, see Fig. 4.



Although TEG degradation could be seen as a drawback, alkoxy and peroxy radicals derived from TEG decomposition might act as damaging agents to microorganisms' membranes.<sup>92,93</sup>

## 4 Conclusions

The dispersion of low concentrations of antimicrobial agents below the exposure limit can be a useful and safe strategy to reduce environmental microorganisms in poor ventilated indoors. We showed that the application of  $\text{O}_3$ ,  $\text{H}_2\text{O}_2$ , and TEG, dispersed individually at safe concentrations, exerts antimicrobial activity on naturally occurring microorganisms and commercial sporulated bacteria. The combination of chemicals can be more effective than the dispersion of the agents alone depending on the combination, microorganism, and environment. The combination of chemicals with oxidant activity was more effective over sporulated bacteria, but not against naturally occurring microorganisms. The combination of compounds with a different mechanism of action was only more effective if TEG was combined with  $\text{O}_3$ , but not with  $\text{H}_2\text{O}_2$ , and only against airborne and surface bacteria. However, the ternary mixture was the most effective against commercial sporulated bacteria and airborne microorganisms. Our results, obtained in a real scenario, support that the dispersion of safe concentrations of agents with antimicrobial activity is a strategy that could reduce airborne transmission diseases in indoors. More research is needed to identify combinable compounds with higher antimicrobial potential to formulate safe antimicrobial mixtures.

## Abbreviations

Triethylene Glycol	TEG
Ozone	$\text{O}_3$
Hydrogen peroxide	$\text{H}_2\text{O}_2$
Electron paramagnetic resonance	EPR
Permissible exposure limit	PELs
Recommended exposure limit	RELS
Time-weighted average concentrations	TWA
Sulfuric acid	$\text{H}_2\text{SO}_4$
Potassium dichromate	$\text{K}_2\text{Cr}_2\text{O}_7$

Nitric acid	HNO <sub>3</sub>
Potassium titanium oxide oxalate dihydrate	C <sub>4</sub> H <sub>2</sub> K <sub>2</sub> O <sub>9</sub> Ti
5,5-Dimethyl-1-pyrroline N-oxide	DMPO
5,5-Dimethyl-1-pyrroline N-oxide over oxidated	DMPOX
2,2,6,6-Tetramethylpiperidine	TEMP
Oxidated 2,2,6,6-tetramethylpiperidine	TEMPO
Colony-forming unit	CFU
Reactive oxygen species	ROS

## Conflicts of interest

There are no conflicts to declare.

## Acknowledgements

Financial support by the Health Research Institute of the Balearic Islands (grant COVID-19/25) and by the Regional Ministry of European funds, University and Culture of the Balearic Islands (grant AP\_2021\_032) is gratefully acknowledged. H. G. B. grant RYC2022-037287-I funded by MICIU/AEI/10.13039/501100011033 and "ESF+".

## References

- 1 K. H. Kim, E. Kabir and S. A. Jahan, Airborne bioaerosols and their impact on human health, *J. Environ. Sci.*, 2018, **67**, 23–35.
- 2 M. I. Guzman, An overview of the effect of bioaerosol size in coronavirus disease 2019 transmission, *Int. J. Health Plann. Manag.*, 2021, **36**(2), 257–266.
- 3 M. Delikhooon, M. I. Guzman, R. Nabizadeh and A. Norouzian Baghani, Modes of Transmission of Severe Acute Respiratory Syndrome-Coronavirus-2 (SARS-CoV-2) and Factors Influencing on the Airborne Transmission: A Review, *Int. J. Environ. Res. Publ. Health*, 2021, **18**(2), 395.
- 4 M. C. de la Rosa, M. A. Mosso and C. Ullán, El aire: hábitat y medio de transmisión de microorganismos, *Obs. Medioambient.*, 2002, **5**, 375–402.
- 5 P. M. Á. Daza, D. X. Martínez Benavides and P. A. Caro Hernández, Contaminación microbiológica del aire al interior y el síndrome del edificio enfermo, *Biociencias*, 2015, **10**(2), 37–50.
- 6 G. Dev Kumar, A. Mishra, L. Dunn, A. Townsend, I. C. Oguadinma, K. R. Bright, *et al.*, Biocides and Novel Antimicrobial Agents for the Mitigation of Coronaviruses, *Front. Microbiol.*, 2020, **11**, 1351.
- 7 M. Oliveira, B. K. Tiwari and G. Duffy, Emerging Technologies for Aerial Decontamination of Food Storage Environments to Eliminate Microbial Cross-Contamination, *Foods*, 2020, **9**(12), 1779.
- 8 C. Gonzalez-Martin. Airborne Infectious Microorganisms. En, editor. *Encyclopedia of Microbiology*, ed. T. M. Schmidt, Academic Press, Oxford, 4th edn, 2019, [citado 13 de noviembre de 2022], pp. 52–60, Disponible en: <https://www.sciencedirect.com/science/article/pii/B978012809633813002X>.
- 9 WHO Coronavirus (COVID-19) Dashboard [Internet], [citado 1 de agosto de 2022], Disponible en: <https://covid19.who.int>.
- 10 J. W. Tang, W. P. Bahnfleth, P. M. Bluyssen, G. Buonanno, J. L. Jimenez, J. Kurnitski, *et al.*, Dismantling myths on the airborne transmission of severe acute respiratory syndrome coronavirus-2 (SARS-CoV-2), *J. Hosp. Infect.*, 2021, **110**, 89–96.
- 11 Z. Peng and J. L. Jimenez, Exhaled CO<sub>2</sub> as a COVID-19 Infection Risk Proxy for Different Indoor Environments and Activities, *Environ. Sci. Technol. Lett.*, 2021, **8**(5), 392–397.
- 12 K. E. Jones, N. G. Patel, M. A. Levy, A. Storeygard, D. Balk, J. L. Gittleman, *et al.*, Global trends in emerging infectious diseases, *Nature*, 2008, **451**(7181), 990–993.
- 13 M. K. Anser, Z. Yousaf, M. A. Khan, A. A. Nassani, S. M. Alotaibi, M. M. Qazi Abro, *et al.*, Does communicable diseases (including COVID-19) may increase global poverty risk? A cloud on the horizon, *Environ. Res.*, 2020, **187**, 109668.
- 14 M. Lidia, A. Joseph, B. William, B. Atze, B. Giorgio, *et al.*, A paradigm shift to combat indoor respiratory infection, *Science*, 2021, **372**(6543), 689–691.
- 15 S. Mosalaei, H. Amiri, A. Rafiee, A. Abbasi, A. N. Baghani and M. Hoseini, Assessment of fungal bioaerosols and particulate matter characteristics in indoor and outdoor air of veterinary clinics, *J. Environ. Sci. Health Environ. Sci. Eng.*, 2021, **19**(2), 1773–1780.
- 16 A. N. Baghani, S. Golbaz, G. Ebrahimzadeh, M. I. Guzman, M. Delikhooon, M. J. Rastani, *et al.*, Characteristics and assessing biological risks of airborne bacteria in waste sorting plant, *Ecotoxicol. Environ. Saf.*, 2022, **232**, 113272.
- 17 A. López, E. Fuentes, V. Yusá, F. X. López-Labrador, M. Camaró, C. Peris-Martínez, *et al.*, Indoor Air Quality including Respiratory Viruses, *Toxic.*, 2021, **9**(11), 274.
- 18 J. Truyols Vives, J. Muncunill, N. Toledo Pons, H. G. Baldov, E. Sala Llins and B. J. Mercader, SARS-CoV-2 detection in bioaerosols using a liquid impinger collector and ddPCR, *Indoor Air*, 2022, **32**(2), e13002.
- 19 T. V. Joan, S. A. Kristiyan, S. L. Ernest, T. P. Nuria, G. B. Herme and M. B. Josep, Efficiency and sensitivity optimization of a protocol to quantify indoor airborne SARS-CoV-2 levels, *J. Hosp. Infect.*, 2022, **130**, 44–51.
- 20 A. Dinoi, M. Feltracco, D. Chirizzi, S. Trabucco, M. Conte, E. Gregoris, *et al.*, A review on measurements of SARS-CoV-2 genetic material in air in outdoor and indoor environments: Implication for airborne transmission, *Sci. Total Environ.*, 2022, **809**, 151137.
- 21 P. Armand and J. Tâche, 3D modelling and simulation of the dispersion of droplets and drops carrying the SARS-CoV-2 virus in a railway transport coach, *Sci. Rep.*, 2022, **12**(1), 4025.
- 22 W. A. Rutala and D. J. Weber, Disinfection, Sterilization, and Control of Hospital Waste. *Mandell, Douglas, and Bennett's Principles and Practice of Infectious Diseases*, 2015, pp. 3294–3309.e4.
- 23 S. N. Rudnick, J. J. McDevitt, M. W. First and J. D. Spengler, Inactivating influenza viruses on surfaces using hydrogen



peroxide or triethylene glycol at low vapor concentrations, *Am. J. Infect. Control*, 2009, **37**(10), 813–819.

24 T. Iwamura, K. Nagano, T. Nogami, N. Matsuki, N. Kosaka, H. Shintani, *et al.*, Confirmation of the Sterilization Effect Using a High Concentration of Ozone Gas for the Bio-Clean room, *Biocontrol Sci.*, 2013, **18**(1), 9–20.

25 B. M. Andersen, M. Rasch, K. Hochlin, F. H. Jensen, P. Wismar and J. E. Fredriksen, Decontamination of rooms, medical equipment and ambulances using an aerosol of hydrogen peroxide disinfectant, *J. Hosp. Infect.*, 2006, **62**(2), 149–155.

26 W. J. Kowalski, W. P. Bahnfleth and T. S. Whittam, Bactericidal Effects of High Airborne Ozone Concentrations on *Escherichia coli* and *Staphylococcus aureus*, *Ozone Sci. Eng.*, 1998, **20**(3), 205–221.

27 K. Rangel, F. O. Cabral, G. C. Lechuga, J. P. R. S. Carvalho, M. H. S. Villas-Boas, V. Middlej, *et al.*, Detrimental Effect of Ozone on Pathogenic Bacteria, *Microorganisms*, 2022, **10**(1), 40.

28 J. Krishnan, N. N. Subhash, C. V. Muraleedharan, P. V. Mohanan, M. Nandakumar, S. Neethu, *et al.*, Chitra Disinfection Gateway for the Management of COVID 19 in Public Entry Places, *Trans. Indian Natl. Acad. Eng.*, 2020, **5**(2), 289–294.

29 B. Bayarri, A. Cruz-Alcalde, N. López-Vinent, M. M. Micó and C. Sans, Can ozone inactivate SARS-CoV-2? A review of mechanisms and performance on viruses, *J. Hazard. Mater.*, 2021, **415**, 125658.

30 C. Tizaoui, Ozone: A Potential Oxidant for COVID-19 Virus (SARS-CoV-2), *Ozone: Sci. Eng.*, 2020, **42**(5), 378–385.

31 T. Pottage, I. Garratt, O. Onianwa, J. Carter and A. M. Bennett, Rapid inactivation of SARS-CoV-2 after exposure to vapour hydrogen peroxide, *J. Hosp. Infect.*, 2021, **118**, 77–78.

32 Y. Cai, Y. Zhao, A. K. Yadav, B. Ji, P. Kang and T. Wei, Ozone based inactivation and disinfection in the pandemic time and beyond: Taking forward what has been learned and best practice, *Sci. Total Environ.*, 2023, **862**, 160711.

33 O. H. Robertson, Disinfection of the air with triethylene glycol vapor, *Am. J. Med.*, 1949, **7**(3), 293–296.

34 C. Elendu Collins, N. Ude. Callistus, E. Odoh Emmanuel and J. Ihedioha Onyedikachi, Natural gas dehydration with triethylene glycol (TEG), *Eur. Sci. J.*, 2015, **11**, 30, <https://url.uk.m.mimecastprotect.com/s/L9-zCoVgyCljYkBf1COEi?domain=eujournal.org>.

35 J. G. Speight, Chapter Seven - Properties Processing of Gas From Tight Formations, En, *Deep Shale Oil and Gas* [Internet], ed. J. G. Speight, Gulf Professional Publishing, Boston, 2017, pp. , pp. 307–347, Disponible en: <https://www.sciencedirect.com/science/article/pii/B9780128030974000073>.

36 R. Jeong, H. Kumar, S. Jones, A. Sandwell, K. Kim and S. S. Park, Increased sanitization potency of hydrogen peroxide with synergistic O<sub>3</sub> and intense pulsed light for non-woven polypropylene, *RSC Adv.*, 2021, **39**(11), 23881–23891.

37 B. Ballantyne and W. M. Snellings, Triethylene glycol HO(CH<sub>2</sub>CH<sub>2</sub>O)3H, *J. Appl. Toxicol.*, 2007, **27**(3), 291–299.

38 Y. Hirama, S. Onishi, R. Shibata, H. Ishida, T. Mori and N. Ota, Antiviral Effect of Propylene Glycol against Envelope Viruses in Spray and Volatilized Forms, *Viruses*, 2023, **15**(7), 1421.

39 R. Jeong, H. Kumar, S. Jones, A. Sandwell, K. Kim and S. S. Park, Increased sanitization potency of hydrogen peroxide with synergistic O<sub>3</sub> and intense pulsed light for non-woven polypropylene, *RSC Adv.*, 2021, **11**(39), 23881–23891.

40 M. Urushidani, A. Kawayoshi, T. Kotaki, K. Saeki, Y. Mori and M. Kameoka, Inactivation of SARS-CoV-2 and influenza A virus by dry fogging hypochlorous acid solution and hydrogen peroxide solution, *PLoS One*, 2022, **17**(4), e0261802.

41 Table Z-1 – Table Z-1. Limits for Air Contaminants. | Occupational Safety and Health Administration [Internet]. [citado 1 de agosto de 2022]. Disponible en: <https://www.osha.gov/laws-regulations/standardnumber/1910/1910.1000TABLEZ1>.

42 CDC – NIOSH Pocket Guide to Chemical Hazards - Hydrogen peroxide [Internet]. [citado 1 de agosto de 2022]. Disponible en: <https://www.cdc.gov/niosh/npg/npgd0335.html>.

43 Hydrogen Peroxide | Occupational Safety and Health Administration [Internet]. [citado 1 de agosto de 2022]. Disponible en: <https://www.osha.gov/chemicaldata/630>.

44 Ozone | Occupational Safety and Health Administration [Internet]. [citado 1 de agosto de 2022]. Disponible en: <https://www.osha.gov/chemicaldata/9>.

45 Hazardous Substance Fact Sheet .pdf [Internet]. [citado 6 de febrero de 2023]. Disponible en: <https://nj.gov/health/eoh/rtkweb/documents/fs/1451.pdf>.

46 Instituto Nacional de Seguridad y Salud en el Trabajo (INSST). Límites de Exposición Profesional 2022 [Internet]. 2022 [citado 6 de febrero de 2023]. Disponible en: <https://bdlep.insst.es/LEP/vlapr.jsp?ID=708&nombre=%C3%93xidodealuminio>.

47 T. Y. Fu, P. Gent and V. Kumar, Efficacy, efficiency and safety aspects of hydrogen peroxide vapour and aerosolized hydrogen peroxide room disinfection systems, *J. Hosp. Infect.*, 2012, **80**(3), 199–205.

48 M. E. Dubuis, N. Dumont-Leblond, C. Laliberté, M. Veillette, N. Turgeon, J. Jean, *et al.*, Ozone efficacy for the control of airborne viruses: Bacteriophage and norovirus models, *PLoS One*, 2020, **15**(4), e0231164.

49 Asociación Española de Normalización, Norma Española UNE-EN ISO 4833-1:2014/A1, 2022.

50 Asociación Española de Normalización, *Norma Española UNE-EN ISO 4833-2:2014/A1*, 2022.

51 Asociación Española de Normalización, *Norma Española UNE-EN ISO 7218*, 2008.

52 Asociación Española de Normalización, *Norma Española UNE-EN ISO 8199* [Internet], BSI British Standards, 2019, Disponible en: <https://linkresolver.bsigroup.com/junction/resolve/000000000030291336?restype=standard>.



53 J. L. Sotelo, F. J. Beltran, F. J. Benitez and J. Beltran-Heredia, Ozone decomposition in water: kinetic study, *Ind. Eng. Chem. Res.*, 1987, **26**(1), 39–43.

54 F. X. Mueller, L. Loeb and W. H. Mapes, Decomposition rates of ozone in living areas, *Environ. Sci. Technol.*, 1973, **7**(4), 342–346.

55 E. S. Shanley and F. P. Greenspan, Highly Concentrated Hydrogen Peroxide, *Ind. Eng. Chem.*, 1947, **39**(12), 1536–1543.

56 Z. M. Galbács and L. J. Csányi, Alkali-induced decomposition of hydrogen peroxide, *J. Chem. Soc., Dalton Trans.*, 1983, (11), 2353–2357.

57 L. J. Heidt and V. R. Landi, Ozone and Ozonide Production and Stabilization in Water, *J. Chem. Phys.*, 1964, **41**(1), 176–178.

58 M. Eriksson, *Ozone chemistry in aqueous solution : ozone decomposition and stabilisation*, 2005 [citado 6 de febrero de 2023]; Disponible en: <http://urn.kb.se/resolve?urn=urn:nbn:se:kth:diva-303>.

59 T. Batakliev, V. Georgiev, M. Anachkov and S. Rakovsky, Ozone decomposition, *Interdiscipl. Toxicol.*, 2014, **7**(2), 47–59.

60 J. Šakalys and R. Girkždienė, Estimation of the ground-level ozone lifetime under rural conditions, *Lith. J. Phys.*, 2010, **50**, 247–254.

61 W. D. Nicoll and A. F. Smith, Stability of Dilute Alkaline Solutions of Hydrogen Peroxide, *Ind. Eng. Chem.*, 1955, **47**(12), 2548–2554.

62 C. C. Lin, F. R. Smith, N. Ichikawa, T. Baba and M. Itow, Decomposition of hydrogen peroxide in aqueous solutions at elevated temperatures, *Int. J. Chem. Kinet.*, 1991, **23**(11), 971–987.

63 P. Pędziwiatr, F. Mikołajczyk, D. Zawadzki, K. Mikołajczyk and A. Bedka, Decomposition of hydrogen peroxide - kinetics and review of chosen catalysts, *Acta Innovations*, 2018, (26), 45–52.

64 C. Houtman and P. Hart, Predicting the Autoaccelerating Hydrogen Peroxide Decomposition Rate after Mixing with Sodium Hydroxide, *Ind. Eng. Chem. Res.*, 2022, **61**(34), 12473–12481.

65 E. Y. Yazıcı, Improvement of Stability of Hydrogen Peroxide using Ethylene Glycol, *J. Sci. Eng.*, 2017, **19**(57), 938–949.

66 Stabilization of aqueous solutions of homo- and copolymers of N-vinylpyrrolidone [Internet]. DE102004049344A1, 2006 [citado 7 de febrero de 2023]. Disponible en: <https://patents.google.com/patent/DE102004049344A1/en>.

67 N. F. Beatty and M. K. Walsh, Influence of thermosonication on *Geobacillus stearothermophilus* inactivation in skim milk, *Int. Dairy J.*, 2016, **61**, 10–17.

68 S. a. Burgess, S. h. Flint and D. Lindsay, Characterization of thermophilic bacilli from a milk powder processing plant, *J. Appl. Microbiol.*, 2014, **116**(2), 350–359.

69 J. McCord, M. Prewitt, E. Dyakova, S. Mookerjee and J. A. Otter, Reduction in *Clostridium difficile* infection associated with the introduction of hydrogen peroxide vapour automated room disinfection, *J. Hosp. Infect.*, 2016, **94**(2), 185–187.

70 R. S. Goglev and M. B. Neiman, Thermal-oxidative degradation of the simpler polyalkyleneoxides, *Polym. Sci.*, 1968, **9**(5), 2351–2364.

71 Y. Nosaka and A. Y. Nosaka, Generation and Detection of Reactive Oxygen Species in Photocatalysis, *Chem. Rev.*, 2017, **117**(17), 11302–11336.

72 G. R. Buettner, Spin Trapping: ESR parameters of spin adducts 1474 1528V, *Free Radic. Biol. Med.*, 1987, **3**(4), 259–303.

73 S. Ortelli, A. L. Costa, P. Matteucci, M. R. Miller, M. Blosi, D. Gardini, *et al.*, Silica modification of titania nanoparticles enhances photocatalytic production of reactive oxygen species without increasing toxicity potential in vitro, *RSC Adv.*, 2018, **8**(70), 40369–40377.

74 J. Hou, L. Xu, Y. Han, Y. Tang, H. Wan, Z. Xu, *et al.*, Deactivation and regeneration of carbon nanotubes and nitrogen-doped carbon nanotubes in catalytic peroxyomonosulfate activation for phenol degradation: variation of surface functionalities, *RSC Adv.*, 2019, **9**(2), 974–983.

75 Y. Liu, C. Chen, X. Duan, S. Wang and Y. Wang, Carbocatalytic ozonation toward advanced water purification, *J. Mater. Chem. A*, 2021, **9**(35), 18994–19024.

76 I. Fenoglio, G. Greco, S. Livraghi and B. Fubini, Non-UV-Induced Radical Reactions at the Surface of TiO<sub>2</sub> Nanoparticles That May Trigger Toxic Responses, *Chem.-Eur. J.*, 2009, **15**(18), 4614–4621.

77 S. Chapman, XXXV. On ozone and atomic oxygen in the upper atmosphere, *London, Edinburgh Dublin Phil. Mag. J. Sci.*, 1930, **10**(64), 369–383.

78 H. Itoh, M. Taguchi and S. Suzuki, Thermal decomposition of ozone at high temperature leading to ozone zero phenomena, *J. Phys. D Appl. Phys.*, 2020, **53**(18), 185206.

79 H. S. Johnston, Global ozone balance in the natural stratosphere, *Rev. Geophys.*, 1975, **13**(5), 637–649.

80 W. H. Glaze, Reaction products of ozone: A review, *Environ. Health Perspect.*, 1986, **69**(7), 151–157.

81 G. Merényi, J. Lind, S. Naumov and S. C. von, Reaction of Ozone with Hydrogen Peroxide (Peroxone Process): A Revision of Current Mechanistic Concepts Based on Thermokinetic and Quantum-Chemical Considerations, *Environ. Sci. Technol.*, 2010, **44**(9), 3505–3507.

82 H. Guo, X. Yu and M. Lin, Kinetic isotope effects in H<sub>2</sub>O<sub>2</sub> self-decomposition: Implications for triple oxygen isotope systematics of secondary minerals in the solar system, *Earth Planet. Sci. Lett.*, 2022, **594**, 117722.

83 F. Haber and J. Weiss, Über die Katalyse des Hydroperoxydes, *Naturwissenschaften*, 1932, **20**(51), 948–950.

84 J. J. Pignatello, E. Oliveros and A. MacKay, Advanced Oxidation Processes for Organic Contaminant Destruction Based on the Fenton Reaction and Related Chemistry, *Crit. Rev. Environ. Sci. Technol.*, 2006, **36**(1), 1–84.

85 A. Hiroki and J. A. LaVerne, Decomposition of Hydrogen Peroxide at Water–Ceramic Oxide Interfaces, *J. Phys. Chem. B*, 2005, **109**(8), 3364–3370.

86 H. Yang, B. Shi and S. Wang, Fe Oxides Loaded on Carbon Cloth by Hydrothermal Process as an Effective and



Reusable Heterogenous Fenton Catalyst, *Catalysts*, 2018, **8**(5), 207.

87 D. A. Armstrong, R. E. Huie, W. H. Koppenol, S. V. Lymar, G. Merényi, P. Neta, *et al.*, Standard electrode potentials involving radicals in aqueous solution: inorganic radicals (IUPAC Technical Report), *Pure Appl. Chem.*, 2015, **87**(11–12), 1139–1150.

88 M. Göltz, M. Koch, R. Detsch, M. Karl, A. Burkowski and S. Rosiwal, Influence of In-Situ Electrochemical Oxidation on Implant Surface and Colonizing Microorganisms Evaluated by Scanning Electron Microscopy, *Materials*, 2019, **12**(23), 3977.

89 J. Glastrup, Degradation of polyethylene glycol. A study of the reaction mechanism in a model molecule: Tetraethylene glycol, *Polym. Degrad. Stab.*, 1996, **52**(3), 217–222.

90 D. B. Min and J. M. Boff, Chemistry and Reaction of Singlet Oxygen in Foods, *Compr. Rev. Food Sci. Food Saf.*, 2002, **1**(2), 58–72.

91 K. K. Høisæter, V. Buvik, S. Villa Gonzalez, S. J. Vevelstad and H. K. Knuutila, Oxidative degradation of triethylene glycol, *Chem. Eng. Sci.*, 2024, **287**, 119706.

92 P. Chaudhary, P. Janmeda, A. O. Docea, B. Yeskaliyeva, A. F. Abdull Razis, B. Modu, *et al.*, Oxidative stress, free radicals and antioxidants: potential crosstalk in the pathophysiology of human diseases, *Front. Chem.*, 2023, **11**, 1158198.

93 S. Matsugo, N. Kayamori, T. Ohta and T. Konishi, Mechanism of Decomposition of Cyclic Peroxides, 4-Alkoxy-1, 4-dihydro-2, 3-benzodioxin-1-ols, to Afford Hydroxyl Radical, *Chem. Pharm. Bull.*, 1991, **39**(3), 545–548.

